NASA TECHNICAL NOTE

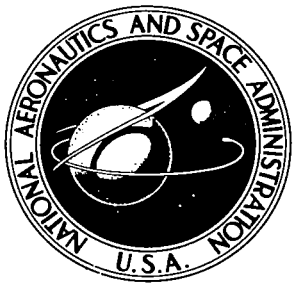

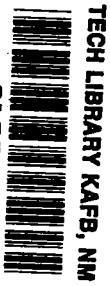

NASA TN D-6652

MAGNETISM, DIMENSIONAL CHANGES, AND MAGNETIC TRANSITIONS IN HYDRATED CESIUM MANGANESE CHLORIDE

by John A. Woollam and Paul R. Aron

Lewis Research Center
Cleveland, Ohio 44135

NATIONAL AERONAUTICS AND SPACE ADMINISTRATION • WASHINGTON, D. C. • FEBRUARY 1972

1. Report No.	2. Government Accession No.	3. Recipient's Catalog No.
NASA TN D-6652		

4. Title and Subtitle	5. Report Date
MAGNETISM, DIMENSIONAL CHANGES, AND MAGNETIC TRANSITIONS IN HYDRATED CESIUM MANGANESE CHLORIDE	February 1972
	6. Performing Organization Code

7. Author(s)	8. Performing Organization Report No.
John A. Woollam and Paul R. Aron	E-6240
	10. Work Unit No. 112-02

9. Performing Organization Name and Address	11. Contract or Grant No.
Lewis Research Center National Aeronautics and Space Administration Cleveland, Ohio 44135	

12. Sponsoring Agency Name and Address	13. Type of Report and Period Covered
National Aeronautics and Space Administration Washington, D.C. 20546	Technical Note
	14. Sponsoring Agency Code

15. Supplementary Notes

16. Abstract

Dimensional changes (strain) along the three principal crystal axes of the antiferromagnet $CsMnCl_3 \cdot 2H_2O$ are studied as a function of magnetic field and temperature in the antiferromagnetic, spin flopped, and paramagnetic phases. Changes in dimensions through the phase transitions between the magnetic states are examined. By applying the molecular field model and utilizing all available information, magnetic properties of $CsMnCl_3 \cdot 2H_2O$ are determined. The possible usefulness of this material in a magnetic refrigeration cycle is evaluated.

17. Key Words (Suggested by Author(s))	18. Distribution Statement
Cesium manganese chloride, Magnetostriction, Thermal expansion, Magnetic properties, Magnetic phase boundaries, Critical performance, Magnetic refrigeration, Antiferromagnet, Spin-flopping, Paramagnetic	Unclassified - unlimited

19. Security Classif. (of this report)	20. Security Classif. (of this page)	21. No. of Pages	22. Price*
Unclassified	Unclassified	22	$3.00

* For sale by the National Technical Information Service, Springfield, Virginia 22151

MAGNETISM, DIMENSIONAL CHANGES, AND MAGNETIC TRANSITIONS IN HYDRATED CESIUM MANGANESE CHLORIDE

by John A. Woollam and Paul R. Aron

Lewis Research Center

SUMMARY

Dimensional changes (strain) along the three principal crystal axes of $CsMnCl_3 \cdot H_2O$ are studied as a function of magnetic field and temperature in the antiferromagnetic, spin flopped, and paramagnetic phases. Changes in dimensions through the antiferromagnetic to spin flopped transition are examined as a function of magnetic field at fixed temperature. Thermal expansion is measured at a fixed field across the antiferromagnetic to paramagnetic and the spin flop to paramagnetic phases. The resultant magnetic phase diagram is plotted. Antiferromagnetic magnetostriction is found to be nearly quadratic in magnetic field. Spin flopped magnetostriction is nearly linear with applied field. Results are compared with predictions of the molecular field model and the magnetic properties are evaluated for possible use in a refrigeration cycle for space applications. An interesting result is an unexplained $\sec^2 \theta$ dependence of the critical field for spin flopping where θ is the angle between magnetic field and the "easy" magnetic axis.

INTRODUCTION

Insulating magnetic materials are of practical interest for a variety of reasons. When an insulator is placed in a changing magnetic field, there are no eddy currents established to shield the magnetic ions in the interior. Thus, for example, refrigeration by adiabatic demagnetization is an important use of these materials, and they are being considered for this use in space applications. To maximize the effectiveness of a material for this use, a maximum value of the Landé spectroscopic splitting factor g and the total spin vector s must be found. In addition, it is important to know the internal exchange and anisotropy fields that cause ordering or disordering of magnetic spins for various temperatures and magnetic fields. In this report the magnetic states of

$CsMnCl_3 \cdot 2H_2O$ are investigated using magnetostriction and thermal expansion. It is found that this is a sensitive method for studying magnetic systems and changes of state. The effectiveness of $CsMnCl_3 \cdot 2H_2O$ is evaluated as a possible refrigerant for space applications.

Magnetostriction is the fractional change $\Delta l/l$ in length l of a material caused by the presence of a magnetic field. This change is called strain and is commonly designated by $\epsilon(=\Delta l/l)$. Magnetostriction effects are large and have been extensively studied in ferromagnets (ref. 1). There have also been some studies of the effects in diamagnetic materials, for example, bismuth (ref. 2). Results on antiferromagnetic CoO were reported by Nakamichi (ref. 3) and on NiO by Belov and Levitin (ref. 4). We have, however, been unable to find any previously reported magnetostriction measurements on spin-flopped antiferromagnets. Preliminary reports of the results of this study were reported in references 5 to 7.

The $CsMnCl_3 \cdot 2H_2O$ crystals grow with plane parallel faces that are parallel to the principal planes of the crystal structure, an ideal configuration for the parallel plate capacitance method (ref. 8) for measuring small changes in length. Another reason why $CsMnCl_3 \cdot 2H_2O$ is an ideal material is that it exhibits spin-flopped antiferromagnetism at conveniently low magnetic fields. In addition, its simple crystal structure makes interpretation of results less difficult.

Magnetic susceptibility (ref. 9) and specific heat (Forstat and McElearney, and Love, unpublished) measurements have shown that there is a one-dimensional antiferromagnetic ordering at temperatures above the Néel temperature of 4.88 K. Specific heat and susceptibility maxima near 20 K suggest that spins aline in linear chains and that the degree of ordering increases for decreasing temperature. At 4.88 K there is a phase transition to a three-dimensional antiferromagnetic state. The magnetic phase boundaries have been determined up to 10 tesla (1 T = 10 kG) by Butterworth and Woollam (ref. 10) and are shown in figure 1.

In figure 2 the crystal morphology is shown, and the axes are labeled. Axes were defined by Jensen, Anderson, and Rasmussen (ref. 11). With a magnetic field smaller than 1.7 tesla and in the $\hat{b}$ direction, the spins aline antiparallel along the $\hat{b}$ direction. Above 1.7 tesla the spins flop from the $\hat{b}$ direction to the perpendicular $\hat{c}$ direction where the spins still are antiferromagnetically ordered. Spin flopping was first predicted by Néel (ref. 12) and later observed by Gorter and Van Peski-Tinbergen (ref. 13) in $CuCl_2 \cdot 2H_2O$. It has its origin in the magnetic anisotropy, which in turn is believed to have its largest contribution from the existence of a spin orbit interaction energy. For a general discussion of spin flopping see Morrish (ref. 14), where a simple molecular field interpretation is given.

SYMBOLS

a, b, c	dimensions of crystal structure
$\hat{a}, \hat{b}, \hat{c}$	orientations of crystal axes
D_1	proportionality constant in antiferromagnetic-paramagnetic boundary theory
E	entropy
$f(\theta)$	function of angle, to be determined
g	magnetic g factor
H	magnetic field
H_A	anisotropy field
H_E	exchange field
H_f	spin flopping field
$H_f(\theta)$	spin flopping field as function of angle
$H_f(O)$	spin flopping field for H parallel to $\hat{b}$
J	exchange energy constant
k	Boltzmann constant
l	length
M	magnetization
m	index of field dependence of volume
n	index of field dependence of strains
s	spin value
T	Néel temperature in field H
T_N	Néel temperature at H = 0
V	volume
ϵ	strain $\left(\epsilon = \frac{\Delta l}{l}\right)$
θ	angle between H and $\hat{b}$ axis
μ_B	Bohr magneton
σ	tension

MAGNETIC STRUCTURE OF $CsMnCl_3 \cdot 2H_2O$

According to Jensen, Anderson, and Rasmussen (ref. 11), the molecular structure is as follows: The crystal structure is orthorhomic with $a = 9.060 \times 10^{-10}$ meter, $b = 7.285 \times 10^{-10}$ meter, and $c = 7.285 \times 10^{-10}$ meter. In figure 3 the unit cell is projected on the $\hat{a}\hat{c}$ plane. The Cl_I link groups with Mn^{++} (spin 5/2) ions at the centers. The Mn^{++} spins can thus be linked into linear chains along the $\hat{a}$ direction, and the Mn^{++} ions on neighboring chains are only weakly linked. The linear chains of spins causes the broad maximum in the susceptibility as found by Smith and Friedberg (ref. 9), and in the specific heat as found by Forstat, McElearney, and Love for temperatures near 20 K. Using a linear chain concept and Fisher's classical Heisenberg model (ref. 15), Smith and Friedberg (ref. 9) found the exchange interaction constant to be $J = -3.0\ k$, where k is the Boltzmann constant. For an Ising model analysis of specific heat data, Forstat, McElearney, and Love find $J = -3.1\ k$. Spence, Jonge, and Rama Rao (ref. 16) find the interchain exchange constants to be $J_1 \cong J_2 \sim 0.04\ k$. Skalyo et al. (ref. 17) have also evaluated J's and find $J \cong 300\ J_1$.

Below 4.8 K the antiferromagnetic ordering is long range. Interchain and intrachain interactions cause three-dimensional ordering with the easy axis of magnetization parallel to the $\hat{b}$ axis.

EXPERIMENTAL METHODS

We use the parallel plate capacitance method developed by White (ref. 8). One plate of the capacitor is glued to the top of the sample and its capacitance with respect to a fixed plate is measured with an ac capacitance bridge (see fig. 4). A lock-in amplifier is used as a null detector and the off-balance voltage is a measure of the strain. The apparatus can detect a strain of 10^{-10} with a one-to-one signal to noise ratio.

Strains perpendicular to the field direction were measured using a split pair superconducting magnet (ref. 18). Strains parallel to the field were measured using a 10-tesla superconducting solenoid. Temperatures down to 1.08 K were achieved by pumping on the liquid-helium bath. Temperatures above 4.2 K were obtained by heating the capacitance cell. Temperatures were measured with a carbon thermometer calibrated against the vapor pressure of He^4.

Crystals of $CsMnCl_3 \cdot 2H_2O$ were grown from a solution of equal parts of CsCl and $MnCl_2 \cdot 4H_2O$. Samples were refrigerated to prevent gain or loss of water over long periods of time. Crystal axes were crudely found by visual observation of the sample morphology (see fig. 2). An accurate determination, within $\pm 0.1^\circ$, was obtained from the symmetry of experimental results as a function of angle.

For all experiments the field was located along or close to the b axis. Strains were then measured in the mutually perpendicular $\hat{a}$, $\hat{b}$, and $\hat{c}$ directions.

EXPERIMENTAL RESULTS

$\hat{c}$ Axis Magnetostriction

In figure 5 the strain along the $\hat{c}$ direction is plotted as a function of magnetic field. In the top half of the figure, the results obtained for a temperature of 1.08 K are shown. The $\hat{c}$ direction strain increases with magnetic field for fields below 1.8 tesla. In this region of field and temperature, the sample is antiferromagnetically ordered as shown by the magnetic phase diagram in figure 1. For fields well below the phase transition ($H < 0.8\ H_f$, where H is magnetic field, H_f is the phase transition field) the field dependence of strain ϵ is

$$\epsilon \propto H^n \tag{1}$$

where $n = 2.0 \pm 0.1$.

At 4.2 K the $\hat{c}$ axis strain has $n = 2.5 \pm 0.1$ but decreases with increasing field below H_c. At the phase transition H_c there is a sharp increase in the $\hat{c}$ dimension for all temperatures. Note, however, that the 4.2 K scale is a factor of ten smaller than the 1.08 K scale.

The sharpness of the strain spike permits accurate identification of the fields for the transition, which are in good agreement with the magnetocaloric results of reference 10. Data for several temperatures is plotted in figure 1. Scatter in these points is due to drift in the integrator used to measure magnetic fields.

Above H_c the field dependence of the strain (fig. 5) did not follow a simple power law. At 1.08 K the strain appeared to saturate to a constant value as a function of field.

In figure 6 the critical field for spin flopping is plotted as a function of angle θ between magnetic field and $\hat{b}$ axis in the $\hat{a}\hat{b}$ plane. These data are found to follow the relation

$$H_f(\theta) = H_f(O)\ \sec^2 \theta \tag{2}$$

to within the accuracy of the experiment, where $H_f(\theta)$ is the critical field for spin flopping at the angle θ.

$\hat{b}$ Axis Magnetostriction

The $\hat{b}$ axis strain is measured parallel to the direction of the magnet field. In figure 7 the strain is plotted as a function of field to 9 tesla at 4.2 K. In this direction for $H < H_f$, n (from eq. (1)) is 2.2±0.1 at 4.2 K. There is little qualitative change in the character of the curve as a function of temperature. At lower temperatures the phase transition peak shifts to lower fields and sharpens. The $\hat{b}$ dimension increases in the antiferromagnetic state and decreases in the spin flopped state. At 4.2 K the $\hat{b}$ strains are larger than the $\hat{c}$ strains shown in figure 5. At low temperatures the $\hat{b}$ strains are several times smaller than the $\hat{c}$ strains.

$\hat{a}$ Axis Magnetostriction

In figure 8 the $\hat{a}$ strain is plotted as a function of magnetic field to 3 tesla for temperatures of 1.24 and 4.2 K. The strain in this direction can also be written

$$\epsilon \propto H^n \tag{3}$$

where at 4.2 K n = 2.2±0.1 and at 1.24 K n = 2.6±0.

Also shown in figure 8 is the dependence of the sharpness of the phase transition spike on the angle between H and the b axis at 4.2 K. The alinement is extremely critical in this orientation since with H only a few degrees from $\hat{b}$ in the $\hat{b}\hat{c}$ plane, the phase transition is very difficult to observe. At 1.24 K the transition is slightly easier to observe. This contrasts with the c axis magnetostriction where the transition was very easy to detect and became more pronounced at low temperatures, and alinement was not critical.

Spin-Flopped Magnetostriction

The field dependence of strain in the spin-flop magnetic state was very temperature and orientation dependent. Thus, for example, figure 5 shows both increasing (4.2 K) and decreasing (1.08 K) strain with field. At 1.08 K the strain is very weakly dependent on field, yet at 4.2 K it is very strongly dependent. In figure 7 strain has a negative slope with increasing field, and in figure 8 the slope is positive. For all three orientations, however, note that the slopes are nearly constant as a function of field even though they are different for different temperatures and orientations.

As shown in figure 1 a change in field at fixed temperatures between 4.36 K (triple point) and 4.88 K (Néel temperature) takes the sample through three phases. At low fields the sample is antiferromagnetic. At intermediate fields it is paramagnetic. And at high fields it is spin flopped-antiferromagnetic. Examples of the strain changes in these three magnetic states are shown in figure 9 for temperatures of 4.67 K and 4.76 K for c axis strains. The knees in the plots of strain as a function of field delineate the phase boundaries for antiferromagnetic to paramagnetic and spin flopped to paramagnetic states. The b axis strains are similarly well defined at the phase boundaries.

A more accurate method of determining the phase boundaries bordering the paramagnetic phase is to fix the magnetic field and heat the sample. The dimensional changes are then a measure of thermal expansion. The thermal expansion shows a knee at the phase boundary as illustrated in figure 10 for c axis strains.

Hysteresis Effects

In the antiferromagnetic to spin-flopped phase transition a hysteresis was observed; that is, the field H_f was not the same for increasing as for decreasing fields. The difference was on the order of 1 percent and was observed for all angles between H and $\hat{b}$ in the $\hat{b}\hat{a}$ plane (c axis magnetostriction) for angles up to 40°. The effect was not studied for angles greater than this.

THEORY AND DISCUSSION

Anisotropy, Exchange, and Spin Flopping

Antiferromagnetism originates in the exchange interaction between ions on different lattice sites. This interaction is a quantum mechanical result of the Pauli exclusion principle. In an antiferromagnetic material the ions are generally further apart than in the ferromagnet so the exchange is usually indirect, through the Cl_I ions (fig. 3) in $CsMnCl_3 \cdot 2H_2O$. Exchange in an antiferromagnet alines spins antiparallel. In a molecular field model these would be pictured as magnetic dipoles each interacting with an equivalent magnetic field, called the exchange field, H_E. A second equivalent field, called the anisotropy field H_A acts to aline spin axes along preferred orientations in particular crystals. These preferred orientations are called easy axes, and the energy necessary to rotate the spins away from the easy direction is called the anisotropy energy. It is the anisotropy that causes spin-flopping and magnetostriction.

In the molecular field model the susceptibility measured parallel to the easy axis is designated by $\chi_{\parallel}$ and that perpendicular by $\chi_{\perp}$. From this model it is easy (ref. 14) to

predict the temperature dependence of susceptibilities, and these are shown in figure 11. The important result is that for $T < T_N$, $\chi_\perp$ is independent of temperature and is greater than $\chi_\parallel$. The free energies associated with these susceptibilities are $-\chi_\perp H^2/2$ and $-\chi_\parallel H^2/2$. Since $\chi_\perp > \chi_\parallel$, the perpendicular spin orientation is energetically favorable for applied magnetic fields above a critical field H_f given by

$$H_f = \left[\frac{2\kappa}{\mu_o(\chi_\perp - \chi_\parallel)}\right]^{1/2} \tag{4}$$

where κ is the anisotropy energy. Above H_f the anisotropy energy is overcome, and the spins flop to the perpendicular orientations.

Smith and Friedberg have measured $\chi_\perp$ and $\chi_\parallel$ as functions of temperature (ref. 9) as shown in figure 12. Later data (unpublished) by Kobayashi and Friedberg shows $\chi_\parallel$ going to zero at $T = 0$ and $\chi_\perp$ to be nearly independent of temperature at low temperatures. At $T = T_N$, $\chi_\perp = \chi_\parallel$ and, at 1 K, $\chi_\perp - \chi_\parallel$ is approximately 0.50 mks/mole (0.040 cgs/mole). Our measured spin flopping field was approximately 1.7 tesla (fig. 1) at 1 K. Thus, from equation (4) κ is 0.57×10^6 joules per cubic meter per mole (5.7×10^6 ergs/cm^3 mole) at 1 K. The temperature dependence of the spin flop boundary is found to be (see fig. 1 and refs. 10 and 19)

$$H_f = (12.8 + 0.814T) \times 10^5 \tag{5}$$

for H_f in ampere-turns per meter and T in kelvin. From reference 9 the susceptibility difference is roughly

$$\chi_\perp - \chi_\parallel = 0.55 \left(1 - \frac{T}{T_N}\right) \frac{\text{mks}}{\text{mole}} \tag{6}$$

The temperature dependence of the anisotropy energy is thus

$$\kappa \simeq 3.49(12.8 + 0.814T)^2 \left(1 - \frac{T}{T_N}\right) \times 10^7 \frac{\text{J}}{(\text{m}^3)(\text{mole})} \tag{7}$$

At 0 K, κ is approximately 0.57×10^6 joules per cubic meter per mole and goes to zero at $T = T_N$. The temperature dependence of H_f reflects the temperature dependence of the spin-wave renormalization, as described by Anderson and Callen (ref. 20).

The angular dependence of the critical field H_f for spin flopping was easily followed in the $\hat{a}\hat{b}$ plane (fig. 6), but flopping did not occur for H more than a few degrees from $\hat{b}$ in the $\hat{b}\hat{c}$ plane (fig. 8). Since spins flop to the $\hat{c}$ direction, they will always flop by 90^o for H in the $\hat{a}\hat{b}$ plane. For H in the $\hat{b}\hat{c}$ plane torques are present that orient

magnetic spins closer to $\hat{c}$ as the field moves away from $\hat{b}$ in the $\hat{b}\hat{c}$ plane. Qualitatively then, the phase transition to $\hat{c}$ is less sharp in the $\hat{b}\hat{c}$ plane, explaining the difficulty in following the transition in the $\hat{b}\hat{c}$ plane. That spins flop to $\hat{c}$ is in agreement with the results of reference 19 but not with the conclusion stated in reference 11.

Skalyo et al. (ref. 17) measured $\chi_\perp$ (c axis) $\simeq 0.52$ mks/mole (0.041 cgs/mole) and $\chi_\perp$ ($\hat{a}$ axis) $\simeq 0.54$ mks/mole (0.043 cgs/mole) as T goes to zero. From the molecular field theory (ref. 22) it is known that

$$H_E H_A = \frac{\kappa}{\chi_\perp} \tag{8}$$

where H_E is the exchange field, and H_A is the anisotropy field. Thus, at 1 K

$$\frac{\kappa}{\chi_\perp} \simeq 1.6T^2 \tag{9}$$

From reference 20 the anisotropy field was found to be 0.048 tesla. Thus, the exchange field in $CsMnCl_3 \cdot 2H_2O$ is approximately 33 tesla. In reference 17 H_A was found to be 0.026 tesla, making H_E approximately 62 tesla.

In figure 1 the spin-flopped to paramagnetic boundary has a nearly vertical slope at 3 tesla. In extremely high fields this transition will move to lower temperatures and will meet the vertical $T = 0$ axis at a field H_p. This field can be estimated from the relation (ref. 21)

$$\mu_B H_p \simeq 2SzJ_1 \tag{10}$$

where S is total spin, J_1 is the exchange constant, and z is the number of nearest neighbors. From reference 9, $J_1 \simeq -3$ k; thus, $H_p \simeq 45$ tesla assuming $z = 2$.

The phase diagram determined by the present measurement is consistent with that found previously (ref. 10). On the antiferromagnetic to spin-flopped boundary the b axis data agree well with reference 10. The errors in the c axis data arise mainly from integrator drift during field measurements. On the spin-flopped to paramagnetic boundary, difficulty in calibrating thermometers was the major source of errors. Systematic differences with the results of reference 10 could also be due to differences of sample alinement.

The antiferromagnetic to spin-flopped antiferromagnetic phase transition has very pronounced effects on strains, as seen in figure 5, for example. This is consistent with this transition being of first order (ref. 21). First-order transitions have associated latent heats, and hysteresis effects could result. With a simple molecular field calculation the hysteresis is not predicted, but Feder and Pytte (ref. 22) show that with a spin

wave theory it is (see also ref. 20). This is a true hysteresis in H_c; that is, it is independent of the rate of change of H for slow changes. Experimentally we observe that the spin-flop transition was on the order of 1 percent higher for decreasing than for increasing fields and existed over a wide range of angles for H in the $\hat{a}\hat{b}$ plane. For H parallel to $\hat{b}$, the hysteresis was also observed by Butterworth and Woollam (ref. 11) over the entire antiferromagnetic - spin-flop boundary.

Using the molecular field approximation, Shapira and Foner find (ref. 23)

$$T_N - T = \frac{g^2 \mu^2 B(2s^2 + 2s + 1)H^2}{40k^2 T_N} \tag{11}$$

for the magnetic field along the easy axis of magnetization, where T_N is the Néel temperature in zero field and T is the antiferromagnetic to paramagnetic transition temperature in a field H. The spin is designated by s, and other quantities have their usual meanings. A plot of

$$T_N - T = D_1 H^2 \tag{12}$$

for our data (supplemented by the data of ref. 11) for H along the easy axis is a good fit with $D_1 = 0.102$ K per square tesla. A least squares polynomial fit shows, however, that higher powers of it may be significant. In $CsMnCl_3 \cdot 2H_2O$ Smith and Friedberg (ref. 9) found a good fit to their susceptibility data using $g = 2.00$ and $s = 5/2$ for the Mn^{++} spins. With this spin, equation (6) predicts $D_1 = 0.255$ K per square tesla, which is more than double that found experimentally. Shapira and Foner found that theory also predicts too large a value for MnF_2 (ref. 23), but in FeF_2 the agreement was quite close (ref. 24).

The $\sec^2 \theta$ dependence of the spin flopping field in the $\hat{a}\hat{b}$ plane is reasonable since symmetry arguments permit only

$$H_f(+\theta) = H_f(-\theta) \tag{13}$$

and

$$H_f(\theta) = H_f(\theta \pm \pi) \tag{14}$$

as also found experimentally. It is easy to argue that H_f should increase as the field moves away from the "easy" axis. The simplest function satisfying these requirements is

$$H_f(\theta) = H_f(0) \sec^2 \theta \tag{15}$$

which is closely followed experimentally.

Magnetostriction

There are two types of magnetostriction, volume and linear (ref. 21). Volume magnetostriction originates in the exchange coupling between magnetic ions. Linear magnetostriction originates in the anisotropy. In both cases it becomes energetically favorable for the lattice to distort in the presence of stress-producing magnetic fields. It should be noted that there is a strong temperature dependence of the anisotropy (eq. (7)), but not for the exchange energy (see however, ref. 18). Thus, the temperature dependent magnetostriction should originate in the magnetic anisotropy. The $\hat{b}$ axis (longitudinal) magnetostriction was nearly independent of temperature, and the $\hat{c}$ axis (fig. 5) magnetostriction had the greatest temperature dependence of the three orientations. In a cubic crystal it should be possible to separate the exchange and anisotropy parts of the strain for each orientation by studying the temperature dependence in each orientation. Thus the total volume change due to exchange could be measured. By symmetry this would be three times the strain due to exchange forces for each direction. This strain could then be subtracted from the measured strain for each direction to get the strain due to anisotropy. Unfortunately, symmetry is not high enough to permit such a separation in $CsMnCl_3 \cdot 2H_2O$. Alternatively, anisotropy fields in cubic antiferromagnets are typically small (ref. 25), thus exchange dominated magnetostriction could be studied directly in cubic systems.

However, the field dependence of volume magnetostriction is of interest, and has been calculated from measurements of individual strains. We find that at 4.2 K for $H < H_f$ the volume increases as

$$\frac{\Delta V}{V} \propto H^m \tag{16}$$

where $m = 2.1 \pm 0.2$ and has a sharp positive spike at the phase transition from antiferromagnetic to spin-flopped states. The large uncertainty in m results from the log-log plot of $\Delta V/V$ as a function of H not being a straight line over all field regions, as is shown by the deviation of the points from a straight line in figure 13. This results from the field dependences of each strain not being identical. That is, n (eq. (1), for example) is not the same for $\hat{a}$, $\hat{b}$, and $\hat{c}$ strains.

Magnetostriction in ferromagnets has been observed and theoretically predicted to be quadratic in magnetic field (refs. 1, 26, and 27). In references 27 and 28 however, only itinerant ferromagnetism is considered. In the work on bismuth (ref. 2), a

diamagnet, it was demonstrated that the magnetostriction was nearly proportional to H^2 and similarly for antiferromagnetic CoO and NiO. The reason for the near quadratic-field dependence of magnetostriction in a variety of types of magnetic materials is not understood. Néel (ref. 28) predicted that the reversible displacement of domain walls is proportional to the square of the magnetic field strength, and Nakamichi (ref. 3) interprets his results from this. There is no evidence in $CsMnCl_3 \cdot 2H_2O$ for a spontaneous magnetostriction, nor a "technical magnetization" (refs. 9 and 14), which would be associated with domain wall displacement. Exchange and anisotropy are probably the major sources of magnetostriction in $CsMnCl_3 \cdot 2H_2O$.

CONCLUDING REMARKS

It is of considerable current interest (ref. 29) to evaluate the possible performance of $CsMnCl_3 \cdot 2H_2O$ for use in a magnetic refrigerator. From simple thermodynamics

$$\left(\frac{\partial T}{\partial H}\right)_E = -\frac{T}{C_H}\left(\frac{\partial M}{\partial T}\right)_H \tag{17}$$

where C_H is the magnetic specific heat measured at fixed field and E is the entropy. Using $M_{\parallel} = \chi_{\parallel} H$ and figure 11, it follows that $\left(\frac{\partial M}{\partial T}\right)_H$ is positive for $T < T_N$. Thus an adiabatically isolated sample will cool in an increasing field since $\left(\frac{\partial T}{\partial H}\right)_E$ is negative. The results of reference 9 show that $\partial M/\partial T$ is still positive for $T > T_N = 4.8$ K (fig. 12) but becomes negative as predicted for a paramagnet (fig. 11) above 20 K. Thus $CsMnCl_3 \cdot 2H_2O$ could be used most effectively to cool for $T < T_N$ and for $H < H_f \simeq 1.7$ tesla (antiferromagnetic state) where $\left|\frac{\partial M}{\partial T}\right|$ is greatest. Between T_N and 20 K it would cool in an increasing field (to any field strength) and would cool in a decreasing field for $T > 20$ K.

To maximize the cooling in the paramagnetic state it is desirable to have a large value of μ_{eff}, where

$$\mu_{eff} = g[s(s+1)]^{1/2} \mu_B \tag{18}$$

In $CsMnCl_3 \cdot 2H_2O$ the g factor is 2.0 and $s = 5/2$. There are four molecular units per chemical cell and the chemical cell has a volume of 755×10^{-30} cubic meter. Thus

$$\mu_{eff} \simeq 3.2 \times 10^{28} \frac{\mu_B}{m^3} \tag{19}$$

For comparison, the effective moment of cerium magnesium nitrate (CMN), a commonly used material, is

$$\mu_{eff} = 0.25 \times 10^{28} \frac{\mu_B}{m^3} \tag{20}$$

The usefulness of CMN results from its desirable ultralow temperature properties. However, this calculation shows that $CsMnCl_3 \cdot 2H_2O$ has a greater density of effective magnetic moments than CMN and could be useful in refrigeration.

Lewis Research Center,
National Aeronautics and Space Administration,
Cleveland, Ohio, November 19, 1971,
112-02.

REFERENCES

1. Callen, Earl; and Callen, Herbert B. · Magnetostriction, Forced Magnetostriction, and Anomalous Thermal Expansion in Ferromagnets. Phys. Rev., vol. 139A, no. 2, July 19, 1965, pp. 455-471.

2. Shoenberg, D.: The Magnetostriction of Bismuth Single Crystals. Proc. Roy. Soc. (London), Ser. A., vol. 150, no. 871, July 1, 1935, pp. 619-637.

3. Nakamichi, Takuro: Magnetostrictive Behavior of Antiferromagnetic CoO Single Crystal in Magnetic Field. J. Phys. Soc. Japan, vol. 20, no. 5, May 1965, pp. 720-726.

4. Belov, K. P.; and Levitin, R. Z.: Magnetostriction of Antiferromagnetic Nickel Monoxide. Soviet Phys. JETP, vol. 10, no. 2, Feb. 1960, pp. 400-401.

5. Woollam, John A.; Aron, Paul R.; and Butterworth, G. J.: Phase Transitions and Magnetostriction in $CsMnCl_3 \cdot 2H_2O$. Bull. Am. Phys. Soc., vol. 16, no. 3, Mar. 1971, pp. 326-327.

6. Aron, P. R.; Woollam, J. A.; and Butterworth, G. J.: Magnetostriction, Thermal Expansion, and Phase Transitions in $CsMnCl_3 \cdot 2H_2O$. Phys. Letters, vol. 35A, no. 6, July 12, 1971, pp. 422-423.

7. Woollam, John A.; and Aron, Paul R.: Phase Transitions and Magnetostriction in $CsMnCl_3 \cdot 2H_2O$. NASA TM X-52997, 1971.

8. White, G. K.: Measurement of Thermal Expansion at Low Temperatures. Cryogenics, vol. 1, no. 3, Mar. 1961, pp. 151-158.

9. Smith, T.; and Friedberg, S. A.: Linear Chain Antiferromagnetism in $CsMnCl_3 \cdot 2H_2O$. Phys. Rev., vol. 176, no. 2, Dec. 10, 1968, pp. 660-665.

10. Butterworth, G. J.; and Woollam, J. A.: Magnetic Phase Diagram of $CsMnCl_3 \cdot 2H_2O$. Phys. Letters, vol. 29A, no. 5, May 19, 1969, pp. 259-260.

11. Jensen, Stig T.; Anderson, Palle; and Rasmussen, Svend E.: The Crystal Structure of $CsMnCl_3 \cdot 2H_2O$. Acta Chem. Scand., vol. 16, no. 8, 1962, pp. 1890-1896.

12. Néel, Louis: Magnetic Properties of the Metallic State and Energy of Interaction Between Magnetic Atoms. Ann. Phys., Ser. 11, vol. 5, 1936, pp. 232-279.

13. Gorter, C. J.; and Van Peski-Tinbergen, Tineke: Transitions and Phase Diagrams in an Orthorhombic Antiferromagnetic Crystal. Physica, vol. 22, 1956, pp. 273-287.

14. Morrish, Allan H.: The Physical Principles of Magnetism. John Wiley & Sons, Inc., 1965.

15. Fisher, Michael E.: Magnetism in One-Dimensional Systems - The Heisenberg Model for Infinite Spin. Am. J. Phys., vol. 32, no. 5, May 1964, pp. 343-346.

16. Spence, R. D.; de Jonge, W. J. M.; and Rama Rao, K. V. S.: Nuclear Resonance Determination of the Magnetic Space Group of $CsMnCl_3 \cdot 2H_2O$. J. Chem. Phys., vol. 51, no. 11, Dec. 1, 1969, pp. 4696-4700.

17. Skalyo, J., Jr.; Shirane, G.; Friedberg, S. A.; Kobayashi, H.; and Tsujikawa, I.: Magnetic Ordering in $CsMnCl_3 \cdot 2H_2O$. Presented at the 12th International Conference on Low Temperature Physics, Kyoto, Japan, 1970.

18. Laurence, James C.: High-Field Electromagnets at NASA Lewis Research Center. NASA TN D-4910, 1968.

19. Botterman, A. C.; de Jonge, W. J. M.; and de Leeuw, P.: Spin-Flopping in $CsMnCl_3 \cdot 2H_2O$. Phys. Letters, vol. 30A, no. 3, Oct. 6, 1969, pp. 150-151.

20. Anderson, F. Burr; and Callen, Herbert B.: Statistical Mechanics and Field-Induced Phase Transitions of the Heisenberg Antiferromagnet. Phys. Rev., vol. 136A, no. 4, Nov. 16, 1964, pp. 1068-1087.

21. Kanamori, Junjiro: Anisotropy and Magnetostriction of Ferromagnetic and Antiferromagnetic Materials. Magnetism. Vol. 1. George T. Rado and Harry Suhl, eds., Academic Press, 1963, pp. 127-203.

22. Feder, J.; and Pytte, E.: Low-Temperature Behavior of the Anisotropic Heisenberg Antiferromagnet in the Neighborhood of the Magnetic Phase Boundaries. Phys. Rev., vol. 168, no. 2, Apr. 10, 1968, pp. 640-654.

23. Shapira, Y.; and Foner, S.: Magnetic Phase Diagram of MnF_2 from Ultrasonic and Differential Magnetization Measurements. Phys. Rev., vol. B1, no. 7, Apr. 1, 1970, pp. 3083-3096.

24. Shapira, Y.: Paramagnetic-to-Antiferromagnetic Phase Boundaries of FeF_2 from Ultrasonic Measurements. Phys. Rev., vol. B2, no. 7, Oct. 1, 1970, pp. 2725-2734.

25. Teaney, Dale T.; Freiser, Marvin J.; and Stevenson, R. W. H.: Discovery of a Simple Cubic Antiferromagnet: Antiferromagnetic Resonance in $RbMnF_3$. Phys. Rev. Letters, vol. 9, no. 5, Sept. 1, 1962, pp. 212-214.

26. Meincke, P. P. M.: Calculation of the Magnetostriction and Thermal Expansion of an Itinerant-Electron Ferromagnet. Can. J. Phys., vol. 48, no. 7, Apr. 1, 1970, pp. 859-861.

27. Meincke, P. P. M.; Fawcett, E.; and Knapp, G. S.: Thermal Expansion and Magnetostriction of $ZrZn_2$. Solid State Comm., vol. 7, no. 22, Nov. 15, 1969, pp. 1643-1645.

28. Néel, Louis: Ferro- and Antiferromagnetism. Proceedings of the International Conference on Theoretical Physics. Kyoto and Tokyo, 1954, pp. 701-714.

29. Brown, G. V.: The Practical Use of Magnetic Cooling. NASA TM X-52983, 1971.

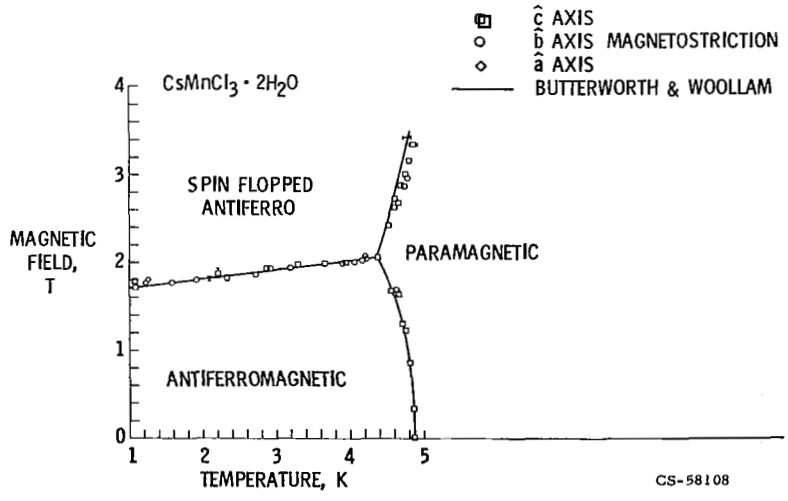

Figure 1. - Magnetic phase diagram for $CsMnCl_3 \cdot 2H_2O$.

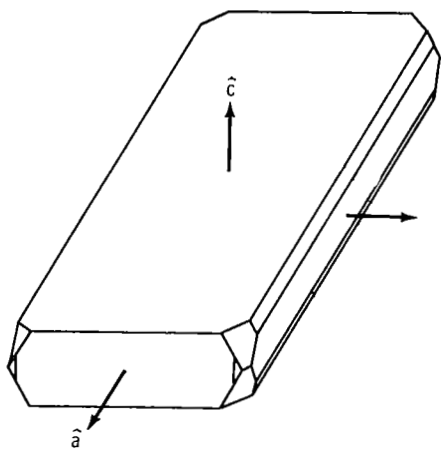

Figure 2. - Crystal morphology showing axes.

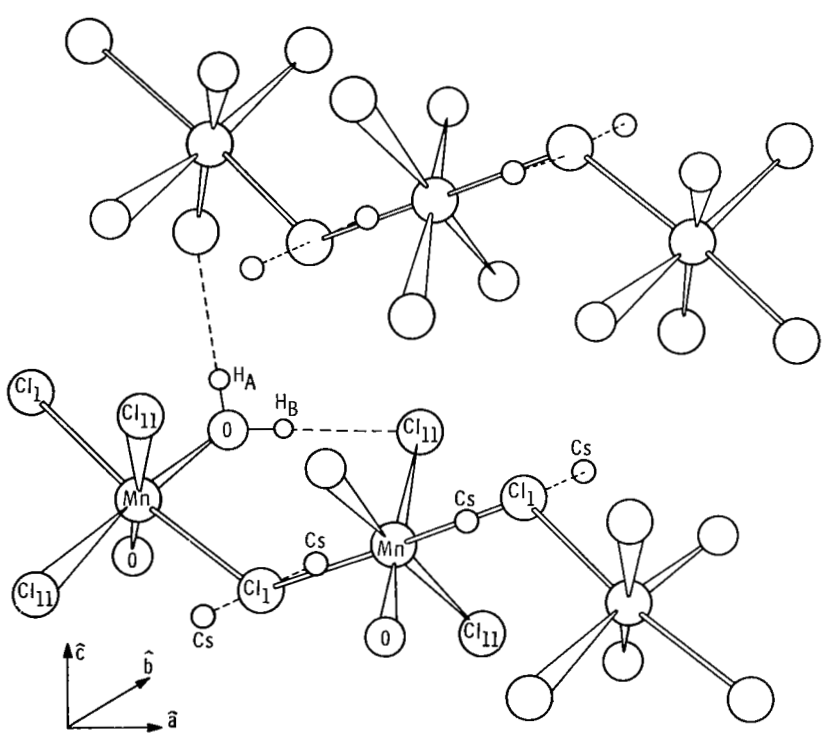

Figure 3. - Molecular structure (refs. 12 and 17) of $CsMnCl_3 \cdot 2H_2O$.

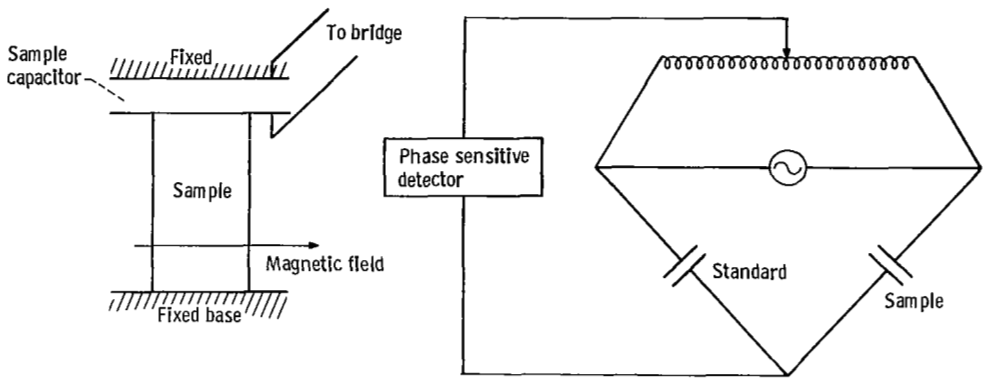

Figure 4. - Magnetostriction and thermal expansion apparatus.

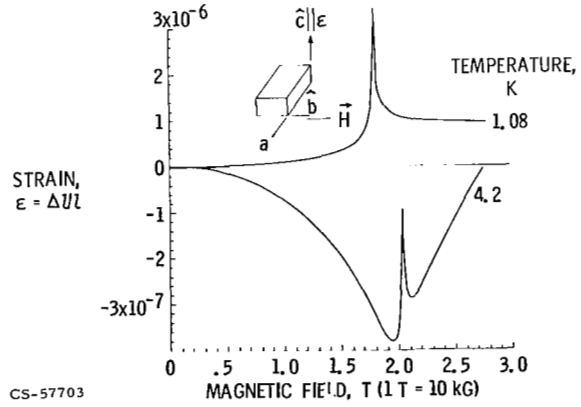

Figure 5. - c axis magnetostriction at 4.2 and 1.08 K.

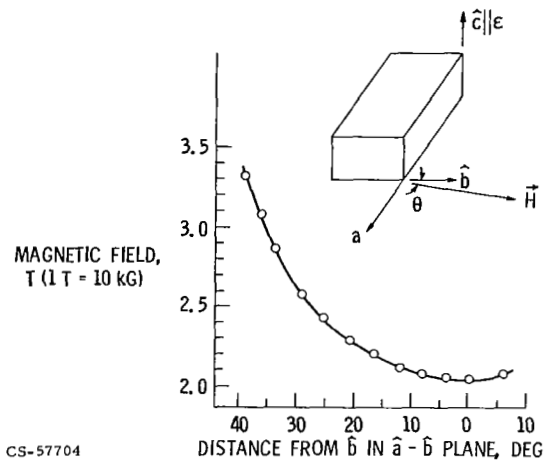

Figure 6. - Critical field for spin flopping as function of angle in the â b̂ plane.

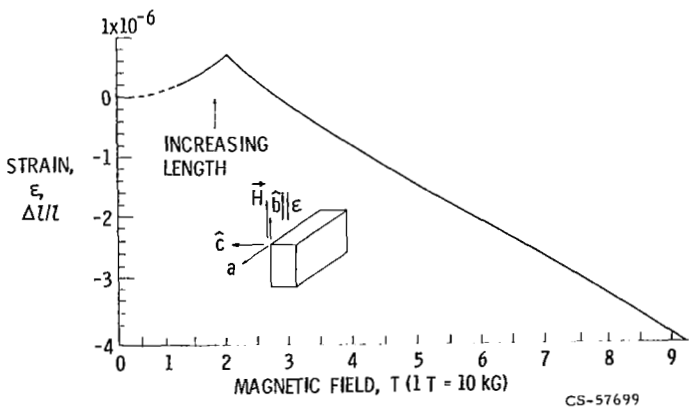

Figure 7. - b axis (longitudinal) magnetostriction at 4.2 K.

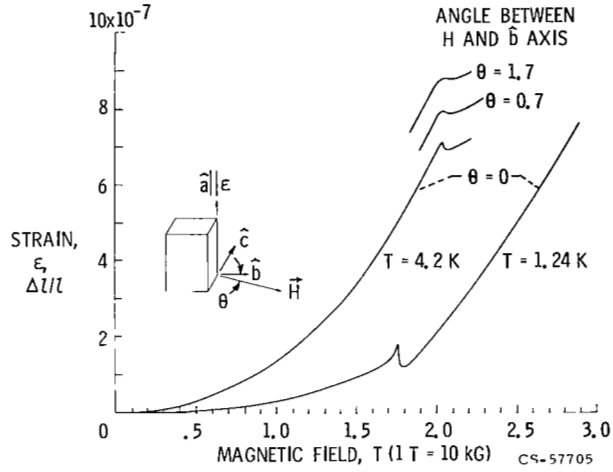

Figure 8. - a axis magnetostriction at 4.2 and 1.24 K.

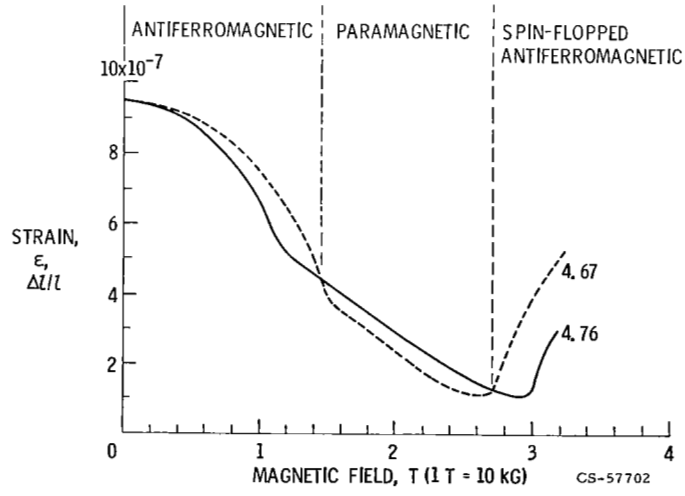

Figure 9. - c axis magnetostriction at 4.76 and 5.67 K showing two phase transitions.

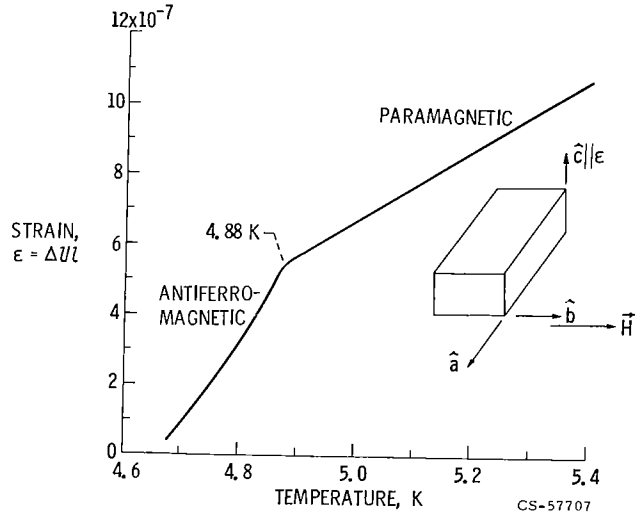

Figure 10. - c axis; zero field thermal expansion.

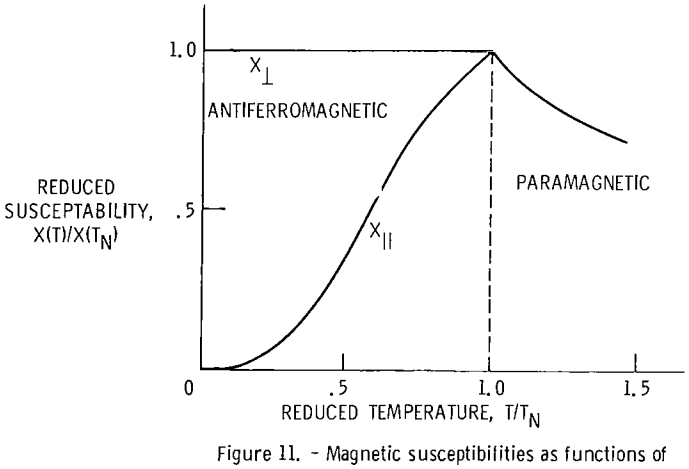

Figure 11. - Magnetic susceptibilities as functions of temperature for an antiferromagnetic as predicted by molecular field model.

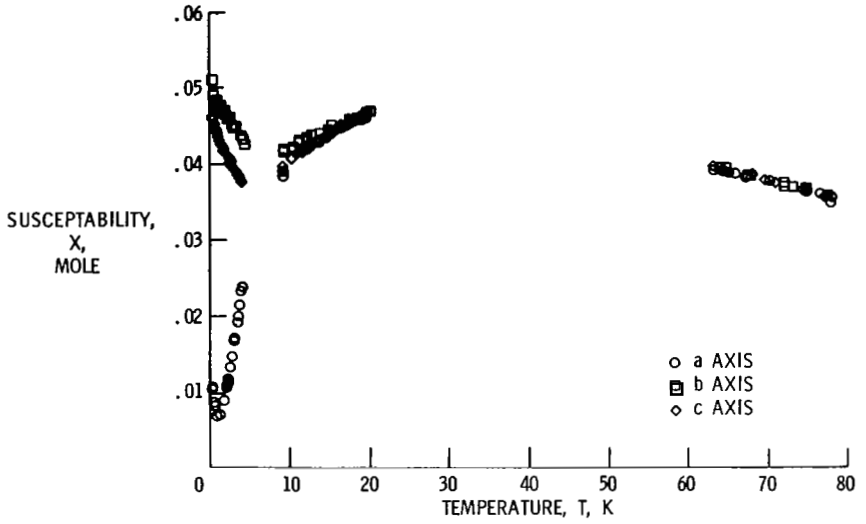

Figure 12. - Magnetic susceptibilities as functions of temperature for $CsMnCl_3 \cdot 2H_2O$ from reference 9.

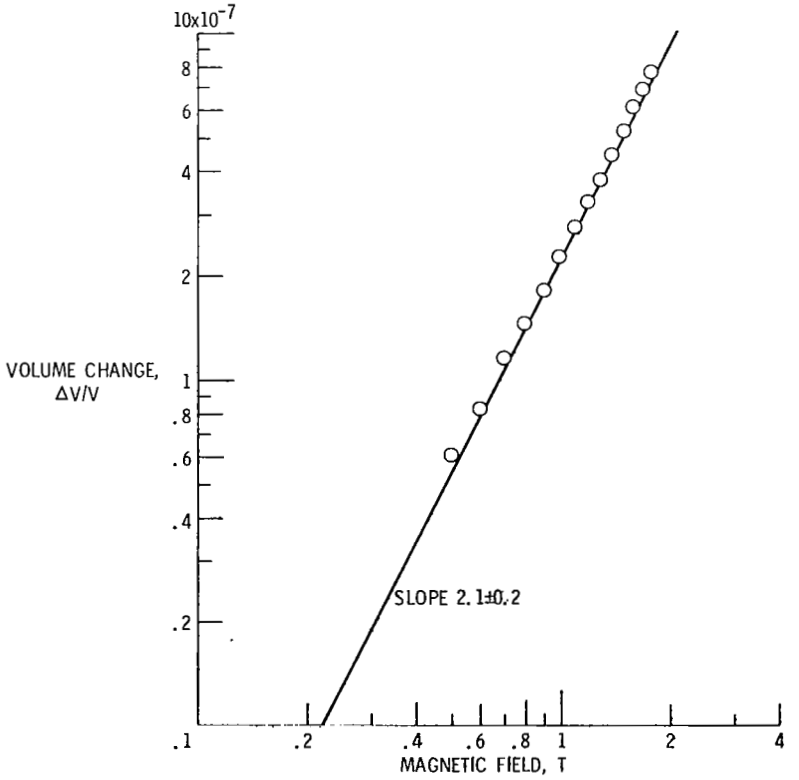

Figure 13. - Log-log plot of volume change as function of field at 4.2 K.